RadioGraphics

When to Suspect Pulmonary Vasculitis: Radiologic and Clinical Clues[1]

CME FEATURE

See accompanying test at http://www.rsna.org/education/rg_cme.html

LEARNING OBJECTIVES FOR TEST 1

After reading this article and taking the test, the reader will be able to:

- Describe the classification and clinical characteristics of the vasculitides.
- List the radiologic, histopathologic, and clinical features of the vasculitides that most frequently affect the respiratory system and the causes of diffuse pulmonary hemorrhage.
- Discuss use of an integrated radiologic and clinical approach for accurate diagnosis.

Eva Castañer, MD • Anna Alguersuari, MD • Xavier Gallardo, MD
Marta Andreu, MD • Yolanda Pallardó, MD • Josep Maria Mata, MD, PhD
José Ramírez, MD

Vasculitis is an inflammatory destructive process affecting blood vessels. Pulmonary vasculitis may be secondary to other conditions or constitute a primary, and in most cases idiopathic, disorder. Underlying conditions in the secondary vasculitides are infectious diseases, connective tissue diseases, malignancies, and hypersensitivity disorders. The most widely used approach to classifying the primary vasculitides is based on the size of the affected vessels (large, medium, small). Thoracic involvement is most commonly seen with primary idiopathic large-vessel vasculitides (Takayasu arteritis, giant cell arteritis, Behçet disease) and primary small-vessel antineutrophil cytoplasmic autoantibody (ANCA)–associated vasculitides (Wegener granulomatosis, microscopic polyangiitis, Churg-Strauss syndrome). The radiologic manifestations of primary pulmonary vasculitis are extremely variable and include vessel wall thickening, nodular or cavitary lesions, ground-glass opacities, and consolidations. Diffuse alveolar hemorrhage is a clinical syndrome that usually results from primary small-vessel vasculitis in the lungs. Although chest radiography is often the first imaging study performed in patients with pulmonary involvement by vasculitis, chest radiographs often fail to show the exact pattern and extent of thoracic involvement and CT is more useful in assessment of the thoracic findings. The pulmonary primary vasculitides are rare disorders, and their diagnoses are among the most demanding challenges in medicine because their signs and symptoms are nonspecific and overlap with those of infections, connective tissue diseases, and malignancies; thus, diagnosis of vasculitis relies on recognition of characteristic combinations of particular clinical, radiologic, laboratory, and histopathologic features.

Abbreviations: ANCA = antineutrophil cytoplasmic autoantibody, CSS = Churg-Strauss syndrome, DAH = diffuse alveolar hemorrhage, FDG = fluorine 18 fluorodeoxyglucose, GCA = giant cell arteritis

RadioGraphics 2010; 30:33–53 • **Published online** 10.1148/rg.301095103 • **Content Codes:** CH CT

[1]From the Department of Radiology, SDI UDIAT-CD, Institut Universitari Parc Taulí–UAB, Corporació Parc Taulí, Parc Taulí s/n, Sabadell 08208 (Barcelona), Spain (E.C., A.A., X.G., M.A., J.M.M.); the Department of Radiology, Hospital de Manises, Valencia, Spain (Y.P.); and the Department of Pathology, Hospital Clínic, Barcelona, Spain (J.R.). Recipient of a Ceritifcate of Merit award for an education exhibit at the 2008 RSNA Annual Meeting. Received April 24, 2009; revision requested May 19 and received July 3; accepted July 13. All authors have no financial relationships to disclose. **Address correspondence to** E.C. (e-mail: *ecastaner@tauli.cat*).

The Editor has no relevant financial relationships to disclose.

Introduction

The term *pulmonary vasculitis* refers to distinct disorders that are pathologically characterized by the destruction of blood vessels (1). Pulmonary vasculitis may be secondary to other conditions or constitute a primary and in most cases idiopathic disorder. Underlying conditions in the secondary vasculitides are infectious diseases, connective tissue diseases, malignancies, and hypersensitivity disorders (2). The primary vasculitides are rare; the overall annual incidence is approximately 20–100 cases per million and the prevalence is 150–450 cases per million (2–4).

The most widely used approach to classifying the primary vasculitides is based on the size of the affected vessels (large, medium, small). We will use this classification because it is useful in suggesting clinical and radiologic features associated with a particular disease. Thoracic involvement is most commonly seen with primary large-vessel vasculitides (Takayasu arteritis, giant cell arteritis [GCA]) and with primary, idiopathic, small-vessel, antineutrophil cytoplasmic autoantibody (ANCA)–associated vasculitides (Wegener granulomatosis, microscopic polyangiitis, and Churg-Strauss syndrome [CSS]) (2).

Diffuse alveolar hemorrhage (DAH) (defined by the presence of hemoptysis, diffuse alveolar infiltrates, and a drop in hematocrit level) is one of the manifestations of primary pulmonary vasculitis, among other entities (idiopathic alveolar hemorrhage, collagen vascular diseases, drug reactions, anticoagulation disorders). Wegener granulomatosis and microscopic polyangiitis are the most common causes of DAH, representing 41% of cases (5).

The clinical approach to pulmonary vasculitis depends on an astute clinician considering the diagnosis and identifying the specific patterns of clinical, radiologic, laboratory, and histopathologic abnormalities.

In this article, we review the classification and clinical characteristics of the vasculitides. We describe the radiologic, pathologic, and clinical features of the primary vasculitides that most frequently affect the thorax. We also discuss the radiologic findings and the underlying causes of DAH. Finally, we emphasize an integrated radiologic and clinical approach for accurate diagnosis.

Table 1
Classification of the Vasculitides

Included in the Chapel Hill nomenclature
Large-vessel vasculitis
GCA
Takayasu arteritis
Medium-sized vessel vasculitis
Polyarteritis nodosa
Kawasaki disease
Small-vessel vasculitis
Wegener granulomatosis*
CSS*
Microscopic polyangiitis*
Henoch-Schönlein purpura
Essential cryoglobulinemic vasculitis
Cutaneous leukocytoclastic angiitis
Not included in the Chapel Hill classification
Primary immune complex–mediated vasculitis
Goodpasture syndrome
Behçet disease
Immunoglobulin A nephropathy
Secondary vasculitis
Classic autoimmune disease
Systemic lupus erythematosus
Rheumatoid arthritis
Polymyositis, dermatomyositis
Scleroderma
Antiphospholipid antibody syndrome
Inflammatory bowel disease
Drug induced
Paraneoplastic
Infection

Source.—References 2, 6, and 7.
*ANCA-associated vasculitis.

Classification

Clinical classification of vasculitis facilitates the diagnosis and management of the disease and enables patients to be assigned to defined groups for clinical studies. The size of the vessels predominantly involved strongly influences the clinical and radiologic features of the different forms of vasculitis and is therefore one major criterion for classification. After the discovery of ANCA, the Chapel Hill consensus conference on the nomenclature of systemic vasculitides elaborated a new classification system, and this is one of the most widely used systems (2,6) (Table 1, Fig 1).

However, the overlap of symptoms and the frequent lack of the full clinical picture limit the

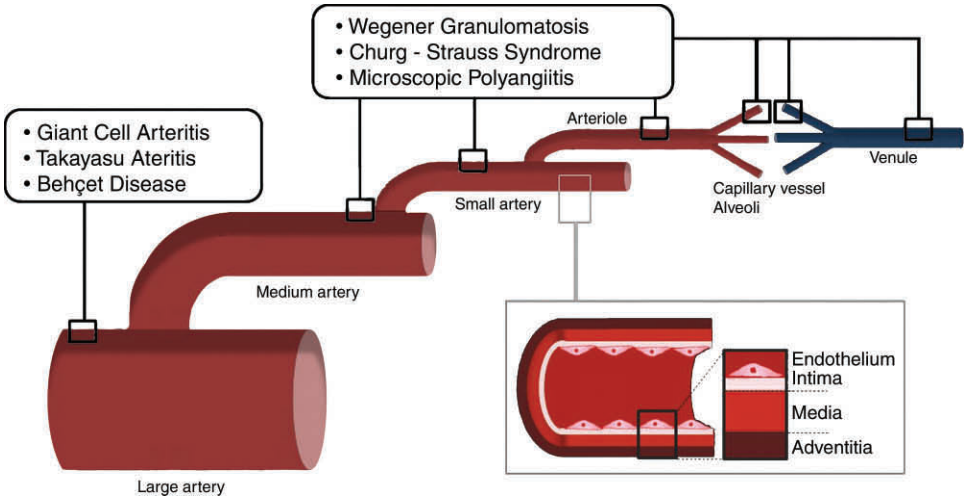

Figure 1. Classification of the primary vasculitides (included in this article) that most frequently affect the respiratory system, according to the size of the predominantly affected vessels. The box on the right shows a normal artery. The large vessels include the aorta and its largest branches; the medium-sized vessels include the main visceral arteries (eg, renal, hepatic, coronary, mesenteric); and the small vessels include the capillaries, venules, and arterioles.

Table 2
Types of ANCA Associated with Primary Small-Vessel Vasculitis

Small-Vessel Vasculitis	Type of ANCA*	Comments
Wegener granulomatosis	c-ANCA (anti-PR3)	85%–90% sensitivity for generalized active Wegener granulomatosis 60% sensitivity for limited pulmonary disease 40% sensitivity for disease in remission
CSS	p-ANCA (anti-MPO)	35%–50% sensitivity
Microscopic polyangiitis	p-ANCA (anti-MPO)	35%–70% sensitivity

Source.—References 9–11.
*anti-MPO = anti-myeloperoxidase, anti-PR3 = anti–proteinase 3, c-ANCA = cytoplasmic ANCA, p-ANCA = perinuclear ANCA.

value of this established vasculitis classification system (8). Thus, the diagnosis of vasculitis relies on the recognition of characteristic combinations of particular clinical, radiologic, laboratory, and histopathologic features. The addition of serologic tests for ANCA along with other immunopathologic markers, such as vascular immunoglobulin A deposits, serum cryoglobulins, and anti–glomerular basement membrane antibodies, facilitates the diagnostic categorization of vasculitis (2).

Teaching Point

ANCAs are antibodies against intracellular antigens found in neutrophils and monocytes. The ANCA-associated vasculitides (Wegener granulomatosis, CSS, and microscopic polyangiitis) are grouped together because of common clinical features, histopathologic involvement of small vessels, similar response to immunosuppressive treatment, and ANCA positivity (9). ANCA positivity is common in these entities but not universal; thus, ANCA negativity does not completely rule out these diseases. Two indirect immunofluorescent staining patterns have been described: cytoplasmic ANCA and perinuclear ANCA (10–12) (Table 2).

Table 3
Clinical and Radiologic Scenarios Suggestive of Vasculitis

Deforming or ulcerating upper airway lesions
Palpable purpura
Mononeuritis multiplex (peripheral neuropathy)
Rapidly progressive glomerulonephritis
Pulmonary-renal syndrome (DAH and glomerulonephritis)
Chest imaging findings of nodular or cavitary diseases
DAH

Source.—References 2 and 9.

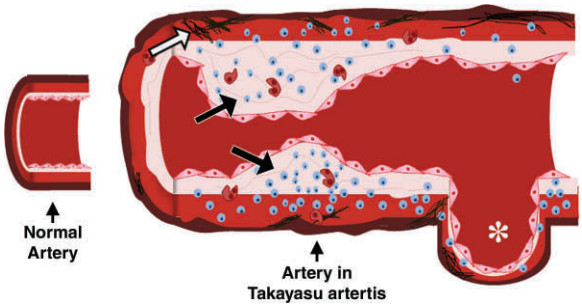

Figure 2. Diagram shows the granulomatous inflammation of the vessel wall that takes place in Takayasu arteritis. Note the marked intimal proliferation (black arrows) and the fibrosis of the media and adventitia (white arrow). These processes lead to segmental stenosis and poststenotic aneurysms (*).

Anti–glomerular basement membrane antibodies should be obtained in all patients with diffuse pulmonary hemorrhage or a pulmonary-renal syndrome; the presence of these antibodies together with both lung and kidney involvement is indicative of Goodpasture syndrome (9).

Clinical and Radiologic Scenarios Suggestive of Vasculitis

Vasculitides are difficult to diagnose because they are uncommon and their signs and symptoms overlap with those of infection, malignancy, thromboembolic disease, and connective tissue diseases (3,4). Large-vessel vasculitis may cause signs and symptoms of ischemia. Nonspecific constitutional signs and symptoms, such as fever, myalgias, arthralgias, and malaise, often accompany small-vessel vasculitis. An unusual constellation of signs and symptoms involving multiple organ systems, either simultaneously or over time, should raise the possibility of a vasculitis. Symptoms such as uveitis, unusual "rashes," arthritis, or "sinus troubles" must be remembered and considered relevant when the clinical presentation is an abnormal finding at chest radiography, shortness of breath, or renal failure (2,9). Moreover, certain clinical scenarios should raise the suspicion of vasculitis (Table 3); these are more frequently associated with ANCA-associated small-vessel vasculitis (9).

Large-Vessel Vasculitis

Large-vessel vasculitides predominantly affect the aorta and its largest branches, such as the major arteries to the extremities and to the head and neck. These vasculitides are suspected when there are signs and symptoms of ischemia. The two major categories are GCA and Takayasu arteritis. Although histologically similar, GCA and Takayasu arteritis are considered distinct disease entities on the basis of the age of onset, distribution of vascular involvement, and clinical presentation (13). Takayasu arteritis affects almost exclusively patients younger than 40 years, involves primarily the aorta and its major branches, and generally spares the cranial arteries. These criteria usually allow clinical differentiation between these two vasculitides. However, more frequent recognition of aortic and large artery involvement in GCA is creating an increasing overlap between these disease entities. Accurate diagnosis of large-vessel vasculitis requires the exclusion of diseases that can mimic vasculitic arterial and aortic disease, such as atherosclerosis.

We also include Behçet disease in this category because it may manifest with similar findings in major arteries.

Takayasu Arteritis

Takayasu arteritis is an idiopathic vascular disorder that may involve the thoracoabdominal aorta and its branches and the pulmonary arteries (14). Although more common in Asia, the disease has been found worldwide, usually affecting young women. Takayasu arteritis is characterized by granulomatous inflammation of the arterial wall with marked intimal proliferation and fibrosis of the media and adventitia; these processes eventu-

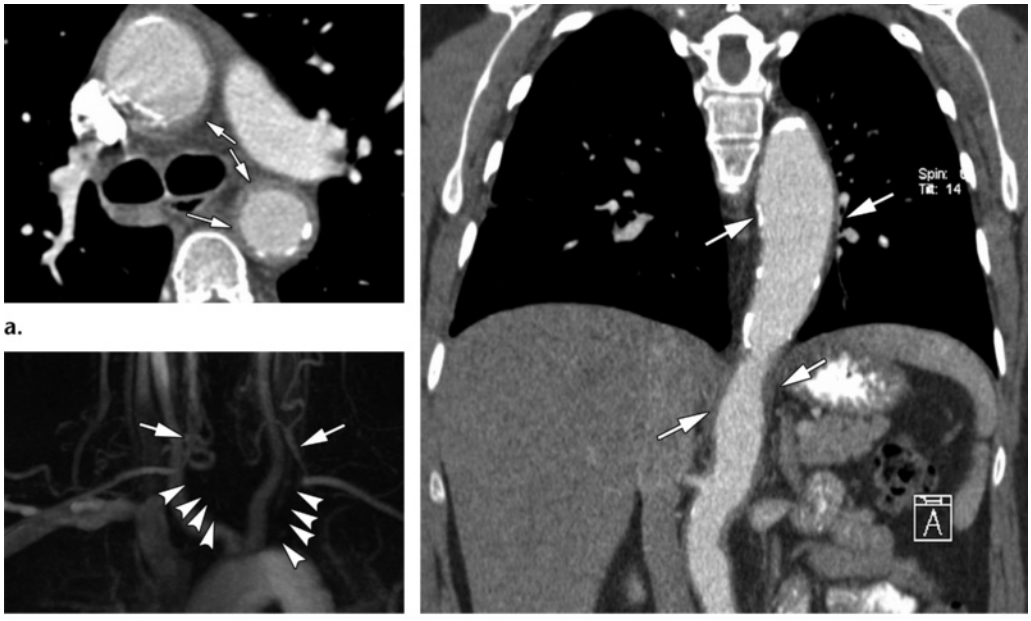

Figure 3. Takayasu arteritis in an asymptomatic 32-year-old woman. Chest CT was performed because of abnormal dilatation of the thoracic descending aorta at chest radiography. **(a)** Contrast-enhanced CT image shows concentric wall thickening of the ascending and descending aorta (arrows) with wall calcifications. **(b)** Oblique coronal reformatted image shows a fusiform aneurysm in the thoracic descending aorta as well as wall thickening of the descending thoracic and abdominal aorta (arrows). **(c)** Maximum intensity projection MR angiogram shows complete occlusion of both prevertebral subclavian arteries (arrowheads); there is collateral flow from the right vertebral artery and left cervical artery (arrows). Both common carotid arteries are patent.

ally lead to stenosis, occlusion, and, occasionally, poststenotic dilatations and aneurysm formation (when inflammation destroys the media) (Fig 2). The lesions tend to be segmental with a patchy distribution (15,16).

The clinical manifestations are usually divided into early and late phases, with a classic triphasic pattern of expression. This consists of an early or prepulseless phase (characterized by nonspecific systemic features, such as low-grade fever, malaise, weight loss, and fatigue), a vascular inflammatory phase, and a late quiescent and occlusive phase; the most common symptom related to vascular stenosis is diminished or absent pulses (96% of patients), typically in association with limb claudication and blood pressure discrepancies (17). However, this sequential presentation is likely to occur only in a minority of patients because the disease is usually recurrent, leading to coexistence of the various phases at one time (17). Symptoms of vascular compromise may be minimized by the development of collateral circulation with the slow onset of stenosis.

Because the clinical presentation and results of laboratory tests are typically nonspecific, accurate diagnosis of Takayasu arteritis virtually always depends on imaging studies. Computed tomography (CT) and magnetic resonance (MR) imaging can provide information on vessel wall thickening in early stages (even before lumen changes become apparent) and on luminal narrowing, aneurysmal dilatation, and occlusion in advanced (fibrotic) stages (Fig 3). However, MR is the imaging modality of choice for assessment of patients suspected or proved to have Takayasu arteritis; it avoids radiation exposure, which is an important consideration in these typically young patients (18). Contrast enhancement of the

thickened walls can be seen with both techniques when some degree of activity is present (19,20).

Pulmonary artery involvement occurs in 50%–80% of patients and is often a late manifestation of the disease. The most characteristic findings are stenosis or occlusion, mainly of the segmental and subsegmental arteries and less commonly of the lobar or main pulmonary arteries (14). CT manifestations of pulmonary artery involvement include wall thickening and enhancement in early phases and mural calcium deposition and luminal stenosis or occlusion in chronic phases (Fig 4). Unilateral occlusion of a pulmonary artery can occur in advanced cases, and late-phase Takayasu arteritis should be considered in cases of chronic pulmonary artery obstruction of unknown origin (14).

Fluorine 18 fluorodeoxyglucose (FDG) positron emission tomography (PET) is a useful indicator of the inflammation of the vessel walls. It is also helpful in follow-up because the intensity of FDG accumulation decreases in response to therapy (21).

Figure 4. Late-stage Takayasu arteritis with pulmonary artery involvement in a 63-year-old woman. Unenhanced CT image shows marked stenosis of the right pulmonary artery (arrowheads), left pulmonary hypertension, and wall calcification of the left pulmonary artery. Calcification of the ascending and descending aorta is also seen. (Case courtesy of Jordi Andreu, MD, Hospital de la Vall d'Hebró, Barcelona, Spain.)

Giant Cell Arteritis

GCA (temporal arteritis) is the most common vasculitis of large and medium-sized arteries, affecting almost exclusively individuals over 50 years of age (22). In this age group, the prevalence of GCA has been estimated at 278 per 100,000 persons in the United States (23), and an even higher frequency has been reported in northern Europe (22). The disease predominantly affects the extracranial carotid branches and the aorta and, rarely, the central pulmonary arteries (7).

Until recently, GCA was believed to be a predominantly localized disease, affecting primarily the cranial arteries, particularly the temporal artery and the arteries of the retina and optic nerve. This pattern of distribution explains many of the classic symptoms of GCA, such as tender and swollen temporal arteries, temporal headache, jaw claudication, and visual loss (24). Another characteristic feature of GCA is the frequent occurrence of systemic and musculoskeletal symptoms. Fatigue, weight loss, low-grade fever, polymyalgia rheumatica, arthralgia, and tenosynovitis are observed alone or in combination in more than one-half of patients with GCA. GCA is increasingly being recognized as a generalized vascular disease potentially leading to serious peripheral arterial complications (24).

Teaching Point

Extracranial involvement is probably underdiagnosed in patients with classic GCA or mistaken for arteriosclerotic disease in patients without temporal arteritis or typical symptoms of GCA. Extracranial GCA has most frequently been reported in the aortic arch and the subclavian and axillary arteries (22,24).

At histologic analysis, GCA appears similar to Takayasu arteritis (24). The principal CT and MR imaging appearance of GCA is similar to that of Takayasu arteritis, with evidence of arterial wall thickening (Fig 5), stenosis, and aneurysm (7). Aortic GCA typically remains asymptomatic during the early phase of the disease and causes serious late complications like aneurysms and dissections. In a retrospective study (25), patients with GCA were 17.3 times more likely to

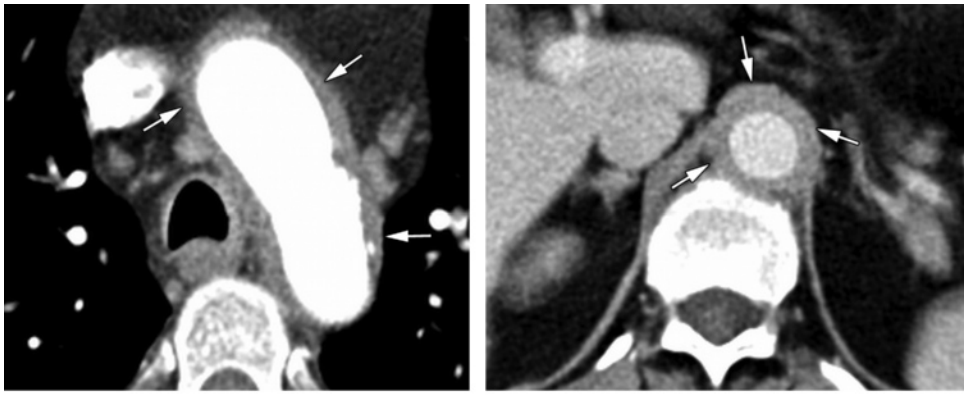

a. b.

Figure 5. GCA in a 72-year-old woman who presented with jaw claudication. Contrast-enhanced CT images show concentric wall thickening (arrows) of the aortic arch **(a)** and abdominal aorta **(b)**.

develop thoracic aortic aneurysms and 2.4 times more likely to develop abdominal aortic aneurysms than individuals of the same age without GCA. Unlike in arteriosclerosis, aneurysms in GCA patients more frequently affect the thoracic aorta and appear to be more prone to dissection (25,26).

As in Takayasu arteritis, FDG PET has an important role in the demonstration of active disease and in follow-up of patients with GCA. However, interpretation of the results is more difficult than in Takayasu arteritis because GCA patients are usually old and frequently have concomitant arteriosclerosis (24), and arteriosclerotic disease causes increased vascular FDG uptake (27). Nevertheless, atherosclerotic lesions can be differentiated from vasculitic lesions by taking into account the vascular distribution, the FDG uptake pattern, and the intensity of FDG accumulation (28).

Behçet Disease

Behçet disease is a chronic multisystemic vasculitis. It is characterized by recurrent oral and genital ulcerations, ocular anomalies (uveitis), and additional clinical manifestations in multiple organ systems. The disease usually manifests in the second or third decade of life, and the male-to-female ratio is reported to be almost equal (29). The reported prevalence of thoracic involvement in Behçet disease ranges from 1% to 8% (29). The vasculitis can involve large, medium, and small vessels of both the arterial and venous circulation (28). Behçet disease associated with lesions in the large vessels is referred to as *vasculo–Behçet disease*, which includes venous or arterial occlusion and aneurysm formation. Systemic arterial manifestations of Behçet disease are infrequent in comparison with venous involvement. The pulmonary arteries are the second most common site of arterial involvement, preceded by the aorta.

Behçet disease is the most common cause of pulmonary artery aneurysm (30); the underlying pathophysiologic process is inflammation of the vasa vasorum of the tunica media with destruction of the elastic fibers and dilatation of the vessel lumen (31). On a chest radiograph, hilar enlargement or a round perihilar area of increased opacity may suggest the presence of an aneurysm (Fig 6a, 6b). Hemoptysis is the most common presenting symptom and is one of the leading causes of death (30). Pulmonary aneurysms in Behçet disease are fusiform to saccular, commonly multiple and bilateral, and located in the lower lobe or main pulmonary arteries (31,32) (Fig 6c). Frequently, in Behçet disease, aneurysms of the pulmonary arteries are partially or totally thrombosed (Fig 6c); the thrombi usually form in situ. In untreated patients, pulmonary

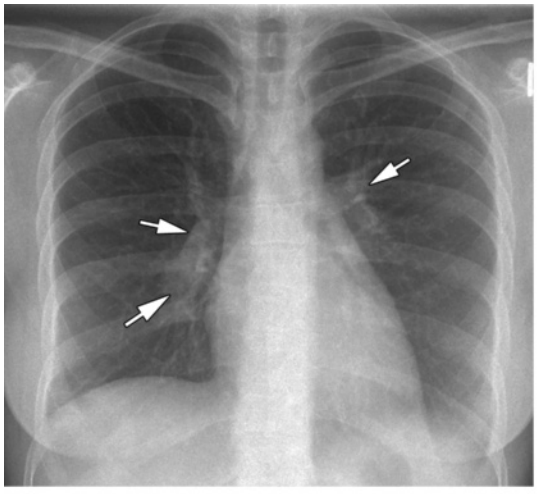

a.

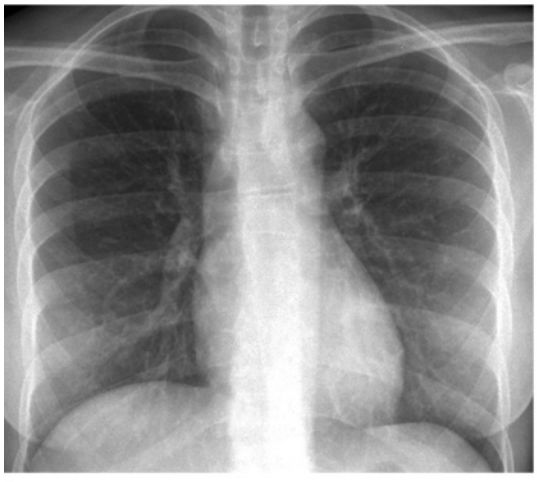

b.

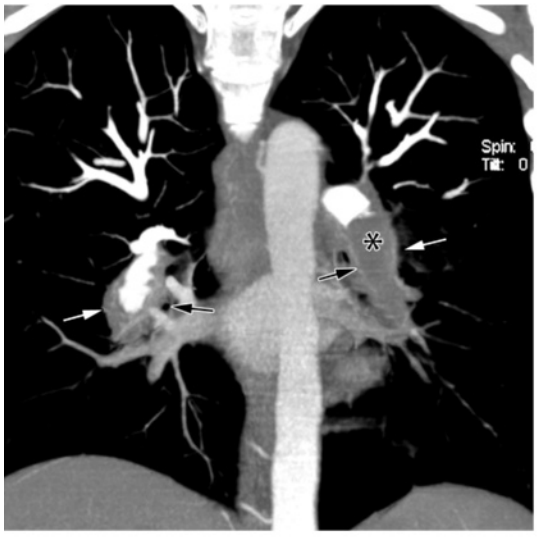

c.

d.

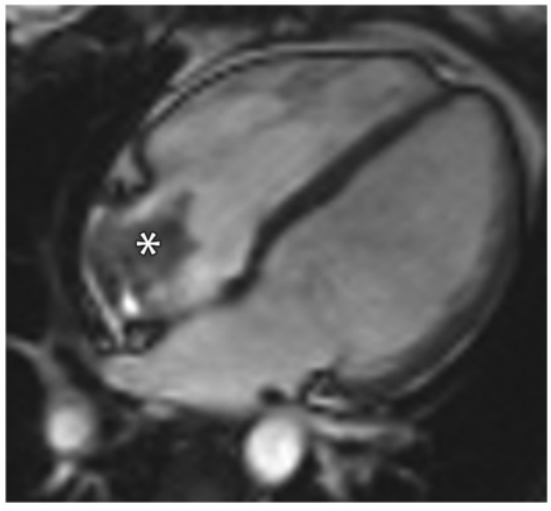

e.

f.

Figure 6. Behçet disease in a 26-year-old woman who presented with dyspnea. **(a)** Chest radiograph shows increased size and opacity of the right interlobar and lower lobe pulmonary arteries as well as of the left pulmonary artery (arrows). **(b)** Chest radiograph obtained 6 months earlier shows normal findings. **(c)** Coronal maximum intensity projection CT image, obtained with 10-mm section thickness, shows increased diameter of both interlobar and lower lobe pulmonary arteries. The aneurysms are thrombosed (arrows), with partial thrombosis on the right and complete thrombosis on the left (*). **(d)** CT image (lung window) shows subpleural wedge-shaped areas of increased opacity, which are suggestive of pulmonary infarction associated with pulmonary thromboembolism. **(e)** T2-weighted MR image (four-chamber view) shows a thrombus in the right atrium (*). **(f)** Coronal maximum intensity projection CT image, obtained with 10-mm section thickness at the same level as in **c** 1 month after immunosuppressive treatment, shows a decrease in the size and in the extent of thrombosis of the bilateral pulmonary artery aneurysms.

aneurysm formation carries a high mortality rate (up to 30% within 2 years; mean patient survival, 10 months from onset of hemoptysis) (29,33). However, there is recent evidence of complete resolution in up to 75% of aneurysms in patients receiving immunosuppressant treatment (7,32) (Fig 6f).

Thickening of the vessel wall due to vasculitis can be seen in the aorta and superior vena cava. Superior vena cava thrombosis, often accompanied by thrombosis of other mediastinal veins, is not uncommon in Behçet disease (30). Intracardiac thrombosis has been described mainly in the right side of the heart (Fig 6e) and often coexists with pulmonary arterial thromboembolism, venous thrombosis, and endomyocardial fibrosis (31,34).

The most common parenchymal lesions are subpleural alveolar infiltrates and wedge-shaped or ill-defined rounded areas of increased opacity, which represent focal vasculitis and thrombosis of pulmonary vessels resulting in infarction (Fig 6d), hemorrhage, and focal atelectasis (30,32).

Medium-sized Vessel Vasculitis

The medium-sized vessels consist of the main visceral arteries (eg, renal, hepatic, coronary, and mesenteric arteries). Polyarteritis nodosa and Kawasaki disease are the two major forms of medium-sized vessel vasculitis. Lung involvement is extremely rare in polyarteritis nodosa, and its presence argues against this entity (35). Kawasaki disease usually occurs in children under 5 years of age (36).

Small-Vessel Vasculitis

Small-vessel vasculitis is defined as vasculitis that affects vessels smaller than arteries, such as arterioles, venules, and capillaries; however, small-vessel vasculitis may also affect arteries, thus overlapping with medium-sized and large-vessel vasculitides (12). The diagnosis of small-vessel vasculitis requires features of vasculitic involvement of capillaries and venules, such as purpura, glomerulonephritis, or pulmonary capillaritis. Lung involvement is most commonly seen with primary, idiopathic, ANCA-associated small-vessel vasculitis.

ANCA-associated small-vessel vasculitides are the most common primary systemic small-vessel vasculitides in adults and include three major categories: Wegener granulomatosis, CSS, and microscopic polyangiitis. Wegener granulomatosis and CSS manifest with necrotizing granulomatous inflammation, whereas microscopic polyangiitis manifests with necrotizing inflammation without granulomatosis (12). These vasculitides can affect people of all ages but are most common in adults 50–69 years of age, and they affect men slightly more frequently than women (12).

Wegener Granulomatosis

Wegener granulomatosis is the most common of the ANCA-associated vasculitides. It is characterized clinically by the triad of upper airway disease (nasal, oral, or sinus inflammation), lower respiratory tract disease (airway or lung), and glomerulonephritis. The complete triad is often not present at initial presentation (9). The upper respiratory tract is affected in almost all patients, and the lungs and kidneys are involved in 90% and 80% of patients, respectively (2,9).

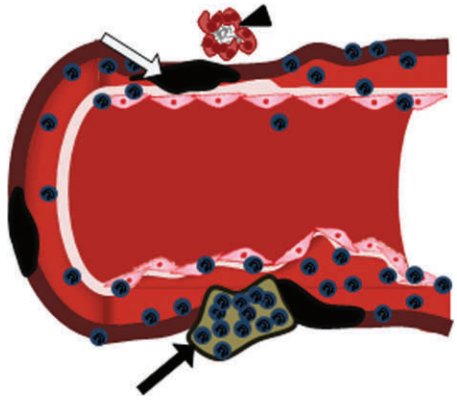

Figure 7. Diagram shows the three major histologic features that characterize Wegener granulomatosis: *(a)* vasculitis with inflammation of medium-sized and small arteries, capillaries, and venules, which are frequently located within inflammatory nodules; *(b)* areas of necrosis (white arrow); and *(c)* necrotizing and nonnecrotizing granulomatous inflammation (arrowhead). In association with the vasculitis, neutrophilic infiltration and microabscess formation (black arrow) may be present.

Other organs less commonly affected include the central and peripheral nervous system, spleen, and large joints. A limited form of Wegener granulomatosis with vasculitis confined to the lung is a well-known variant and usually precedes systemic manifestations (7,37). Pulmonary symptoms include hemoptysis, cough, chest pain, and dyspnea. Tracheobronchial involvement is seen in 10%–55% of patients and causes stridor, dyspnea, and postobstructive pneumonia. The most common manifestations of upper airway involvement are rhinorrhea, epistaxis, sinusitis, otitis, and sometimes destructive bone lesions (12).

Chest radiographs fail to show the pattern and distribution of thoracic disease sufficiently, and CT is more sensitive for detection of lung involvement.

Nodules, Masses, and Consolidation.—At histopathologic analysis, nodules and masses in active pulmonary disease are composed of granulomatous tissue (38). The characteristic granulomas of Wegener granulomatosis are confluent necrotizing lesions with a tendency toward cavitation (38) (Fig 7). The most common radiographic and CT abnormalities, seen at presentation in up 90% of patients, consist of lung nodules and masses (Fig 8) (39,40). The nodules and masses are usually multiple and bilateral; they tend to involve mainly the subpleural regions or less commonly the peribronchovascular regions but have no predilection for the upper or lower lung zones. The nodules and masses may have smooth or, less commonly, irregular margins (Fig 8).

With progression of disease, nodules and masses tend to increase in size and number, sometimes coalescing (Fig 8), and can range from a few millimeters to more than 10 cm in diameter. At CT, most nodules larger than 2 cm are cavitated. Cavities are usually thick walled with an irregular inner margin, but they may become thin walled and decrease in size with treatment (Fig 8) (39,40). The CT halo sign (a rim of ground-glass opacity surrounding the pulmonary lesion) is seen in up to 15% of cases (41). On contrast-enhanced CT scans, most noncavitated nodules or masses show central low attenuation with or without peripheral enhancement; low attenuation may reflect extensive necrosis (Fig 9) (38).

Approximately 50% of the nodules and masses resolve in response to treatment, 40% diminish in size (leaving significant residual damage) (Fig 8f), and 10% remain unchanged (41,42).

Airspace consolidations and patchy or less commonly diffuse ground-glass opacities are the second most common radiographic finding (20%–50% of cases) and may occur with or without associated lung nodules and masses. The consolidations and ground-glass opacities reflect either vasculitic pulmonary disease in the form of pneumonitis or alveolar hemorrhage (41,43). The areas of

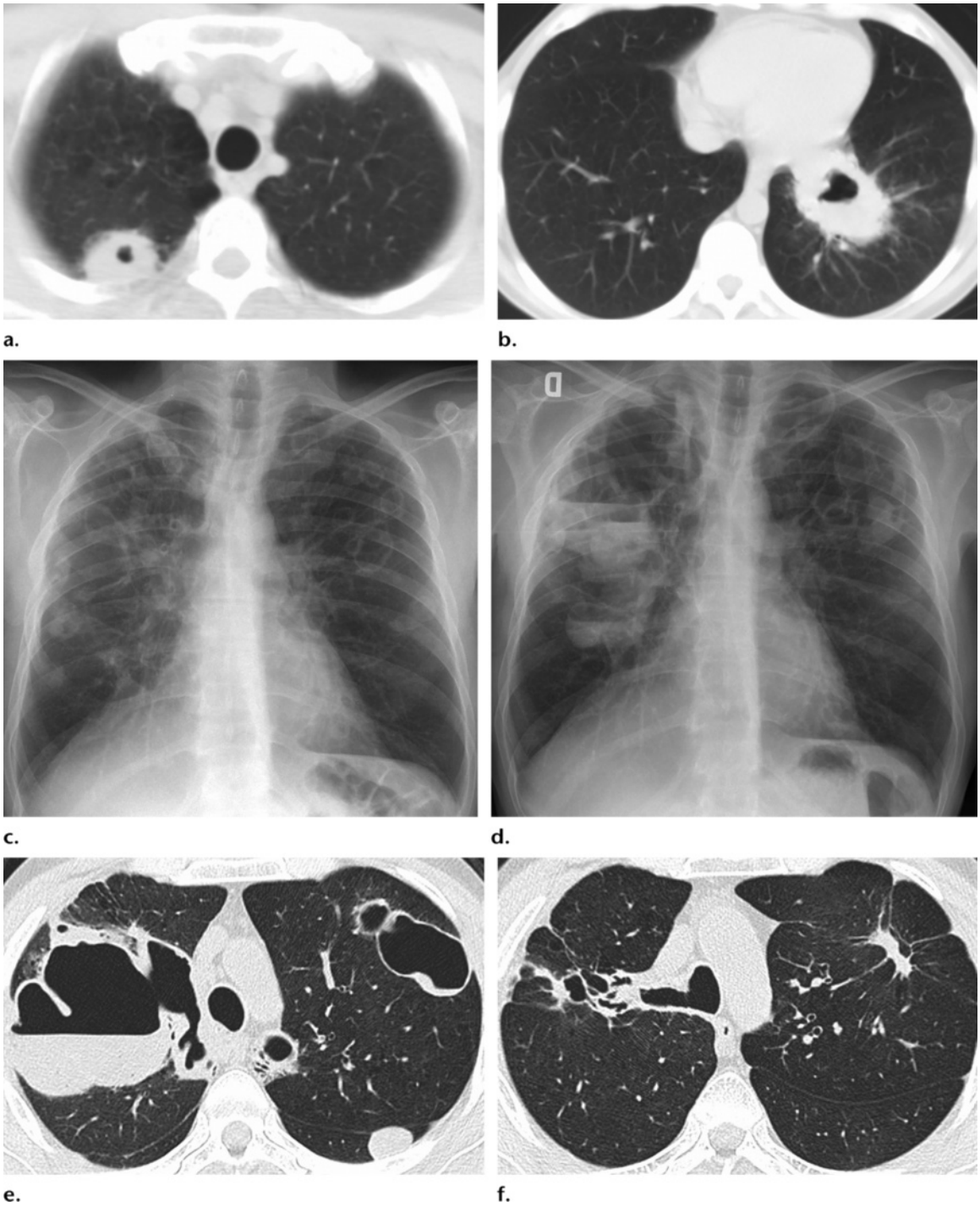

Figure 8. Relapsing Wegener granulomatosis in a 57-year-old man who initially presented with malaise and recurrent episodes of epistaxis. **(a, b)** CT images (lung window) show irregular, thick-walled, cavitated masses in the right upper lobe **(a)** and left lower lobe **(b)**. The patient responded satisfactorily to treatment, with complete resolution of the pulmonary masses. Two years later, the patient presented with arthralgias and hemoptysis. **(c)** Posteroanterior chest radiograph shows well-defined multiple bilateral nodules, some of which are cavitated, affecting predominantly the upper lobes. Despite immunosuppressive treatment, 3 months later the patient presented with acute shortness of breath and a cough. **(d)** Chest radiograph shows coalescence of the cavitated lesions, some of which demonstrate an air-fluid level secondary to infection. **(e)** CT image (lung window) shows bilateral fairly well-defined nodules and masses. Some lesions are cavitated and demonstrate air-fluid levels. Some of the cavities are thin walled. **(f)** CT image (lung window) obtained 1 year later shows a favorable response to treatment, with marked fibrotic reaction around the healing residual lesions.

consolidation may have a random distribution, appear as peripheral wedge-shaped lesions mimicking pulmonary infarcts, or have a peribronchial distribution (Fig 10a, 10b). Diffuse ground-glass bilateral opacities represent alveolar hemorrhage. DAH occurs in approximately 10% of patients with Wegener granulomatosis (44).

Tracheobronchial Involvement.—Bronchial abnormalities (once regarded as an unusual CT finding), mainly bronchial wall thickening in the segmental and subsegmental bronchi (Fig 10c), have been reported in 40%–70% of patients (39). Bronchiectasis is seen less frequently (10%–20%) (40,41). Large airway involvement may be focal or diffuse. Concentric tracheal wall thickening due to inflammation with narrowing of the airway lumen is present in 15% of patients (39). Involvement of the subglottic trachea is most typical, with variable involvement of the vocal cords, distal trachea, and proximal main-stem bronchi (42). Bronchial wall involvement may lead to airway obstruction and atelectasis.

Recurrent Wegener granulomatosis in the lung may appear similar to the initial presentation or may appear with different patterns from those seen at initial presentation (Fig 8) (39).

The main radiologic differential diagnoses for Wegener granulomatosis (essentially bilateral subpleural nodules or masses) include infections (septic embolism, multiple abscesses), neoplasms (hematogenous metastases, lymphoma), and organizing pneumonia, as well as Kaposi sarcoma when peribronchovascular lesions predominate.

The fast changes (occurring in days or a few weeks) that nodules and masses in Wegener granulomatosis demonstrate argue against malignancy.

Wegener granulomatosis can usually be distinguished from these other conditions clinically by the presence of upper respiratory symptoms, laboratory findings indicative of glomerulonephritis, and the presence of cytoplasmic ANCA in serum (seen in 90% of patients with active disease) (45).

Churg-Strauss Syndrome

CSS is characterized by the clinical triad of asthma, hypereosinophilia, and necrotizing vasculitis (35). The diagnosis of CSS can be made if four or more of the following six findings are present: asthma, more than 10% eosinophilia in a differential white blood cell count, mononeuropathy or polyneuropathy attributable to systemic vasculitis, migratory or transient pulmonary opacities, paranasal sinus abnormalities, and extravascular eosinophils in a biopsy specimen (46). Relatively late age of onset (mean, 32 years) distinguishes the asthma in CSS from asthma in the general population (47). The lung is the most commonly involved organ, followed by the skin. Pulmonary hemorrhage and glomerulonephritis are much less common than in the other small-vessel vasculitides (47). The heart is a primary target organ in CSS, and coronary arteritis and myocarditis are the main causes of morbidity and mortality (48).

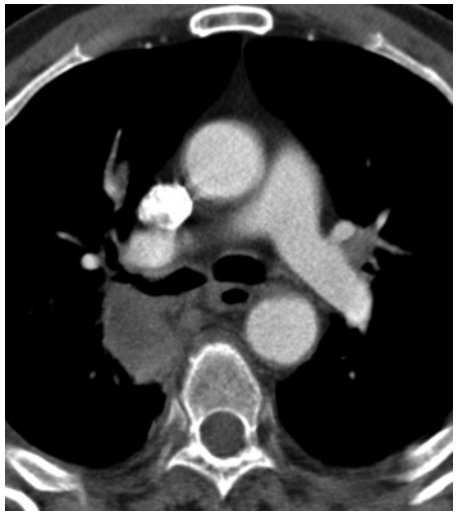

Figure 9. Wegener granulomatosis in a 76-year-old man who presented with otitis and arthralgias. Contrast-enhanced CT image shows a mass in the right lower lobe with a central low-attenuation area. The patient also had other bilateral noncavitated masses (not shown).

At histopathologic analysis, both necrotizing small-vessel vasculitis and an eosinophil-rich inflammatory infiltrate with necrotizing granulomas are seen (49) (Fig 11).

Clinically, CSS shows three distinct phases: *(a)* a prodromal phase that may persist for many years, consisting of asthma and often preceding allergic rhinitis; *(b)* a phase of marked peripheral blood eosinophilia and eosinophilic tissue infiltrates; and *(c)* a life-threatening vasculitic phase (50). However, these phases do not always manifest in this order. The first two phases are

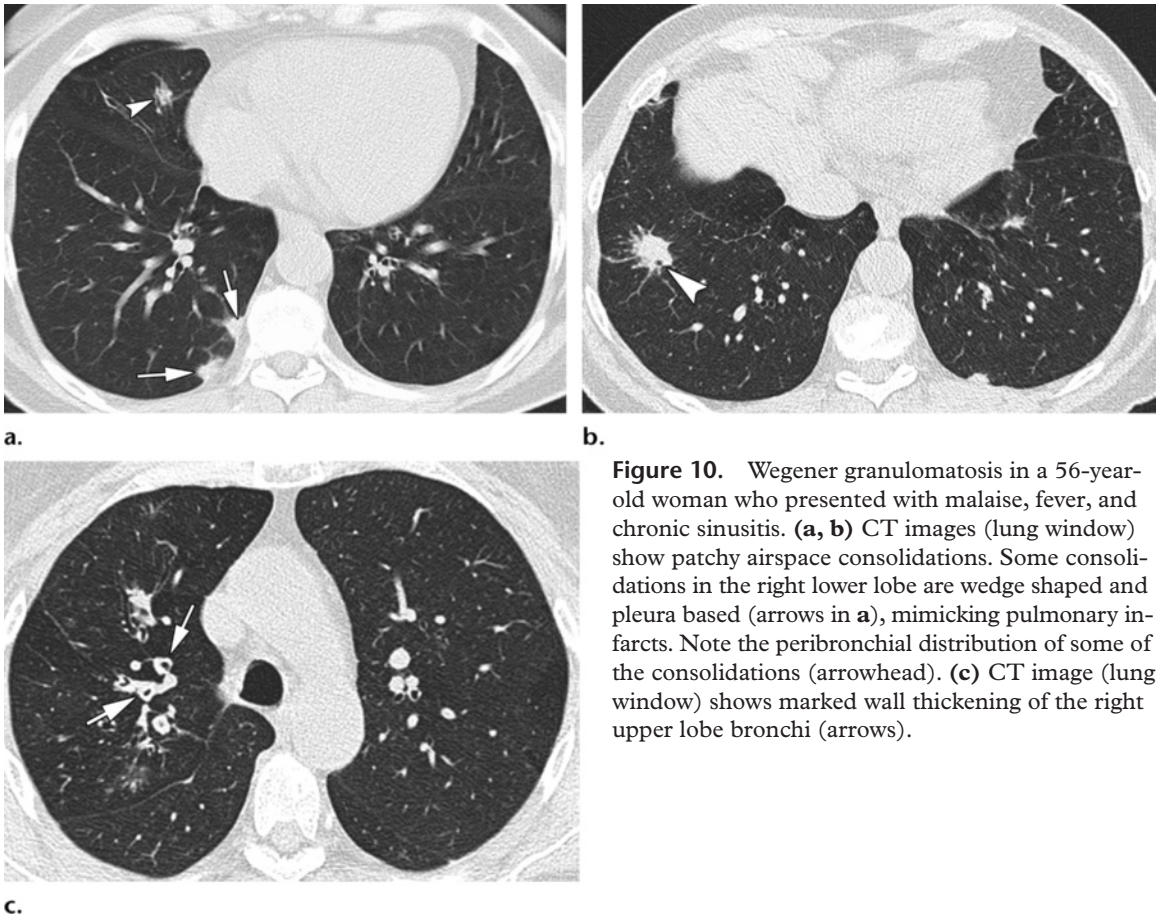

Figure 10. Wegener granulomatosis in a 56-year-old woman who presented with malaise, fever, and chronic sinusitis. **(a, b)** CT images (lung window) show patchy airspace consolidations. Some consolidations in the right lower lobe are wedge shaped and pleura based (arrows in **a**), mimicking pulmonary infarcts. Note the peribronchial distribution of some of the consolidations (arrowhead). **(c)** CT image (lung window) shows marked wall thickening of the right upper lobe bronchi (arrows).

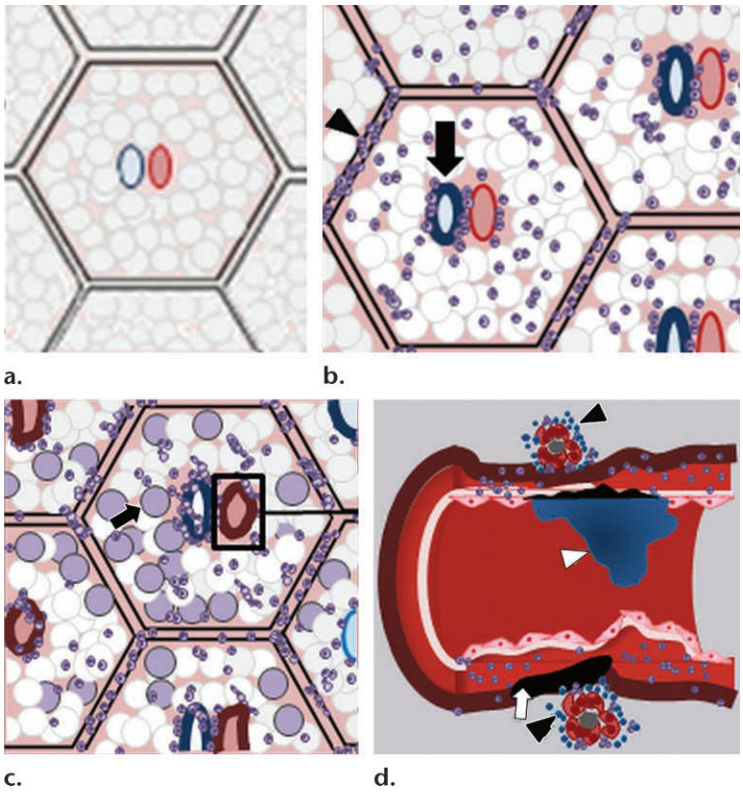

Figure 11. Main histologic features of CSS. Diagrams show the normal secondary pulmonary lobule **(a)**, the secondary pulmonary lobule in the prodromal stage **(b)**, eosinophilic infiltration of the alveoli (arrow in **c**), and the vasculitic phase **(d)**. In **a–c**, the bronchus (blue oval) and artery (red oval) are seen in the middle of the lobule; the white circles represent the alveoli. In the prodromal stage, bronchiolitis with eosinophilic and neutrophilic infiltration of the bronchial wall (arrow in **b**) and septal infiltration by eosinophils (arrowhead in **b**) can be seen. Once the vasculitic phase is established, granulomatous necrosis of medium-sized arteries, veins, and capillaries is apparent. Extravascular granulomas (black arrowheads in **d**), fibrinoid necrosis (arrow in **d**), and thrombosis (white arrowhead in **d**) are common findings.

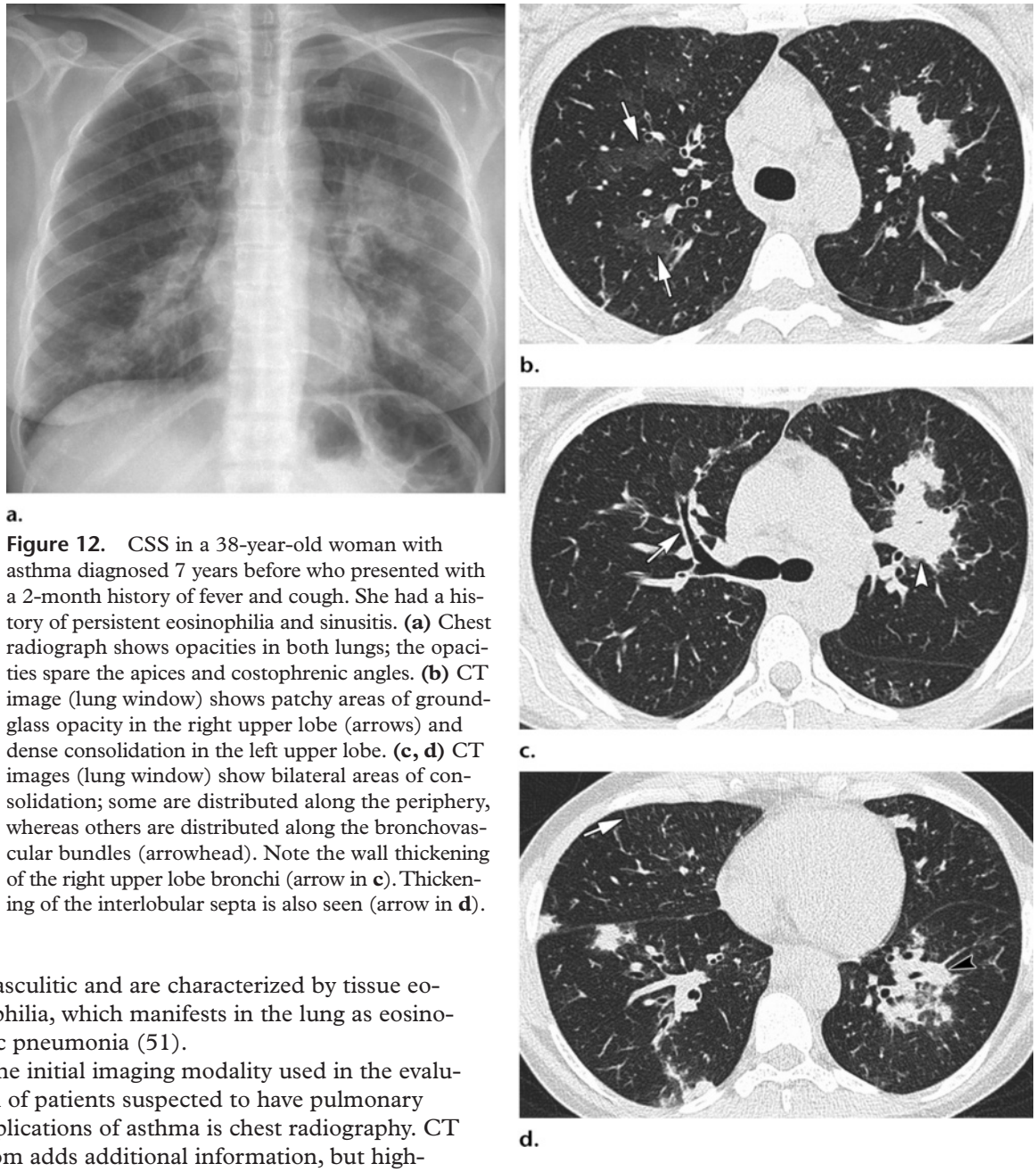

a.

b.

c.

d.

Figure 12. CSS in a 38-year-old woman with asthma diagnosed 7 years before who presented with a 2-month history of fever and cough. She had a history of persistent eosinophilia and sinusitis. **(a)** Chest radiograph shows opacities in both lungs; the opacities spare the apices and costophrenic angles. **(b)** CT image (lung window) shows patchy areas of ground-glass opacity in the right upper lobe (arrows) and dense consolidation in the left upper lobe. **(c, d)** CT images (lung window) show bilateral areas of consolidation; some are distributed along the periphery, whereas others are distributed along the bronchovascular bundles (arrowhead). Note the wall thickening of the right upper lobe bronchi (arrow in **c**). Thickening of the interlobular septa is also seen (arrow in **d**).

prevasculitic and are characterized by tissue eosinophilia, which manifests in the lung as eosinophilic pneumonia (51).

The initial imaging modality used in the evaluation of patients suspected to have pulmonary complications of asthma is chest radiography. CT seldom adds additional information, but high-resolution CT is indicated when radiographic findings are questionable or nonspecific.

The most common lung radiographic manifestations of CSS consist of transient, bilateral, nonsegmental areas of consolidation without predilection for any lung zone (51) (Fig 12a). The areas of consolidation can be transient, resembling Löffler syndrome, or predominantly peripheral (50% of cases), resembling chronic eosinophilic pneumonia or organizing pneumonia (52,53). The most common abnormality at high-resolution CT, seen in up to 90% of patients, is bilateral areas of ground-glass opacity or consolidation (Fig 12) (47,52). These usually have a symmetric distribution and often a peripheral predominance; less commonly, they have a peribronchial or patchy random distribution (51,52). Another relatively common finding is the presence of septal lines, seen in approximately 50%

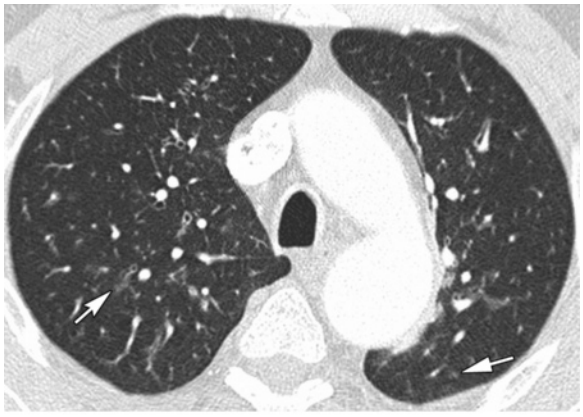

a.

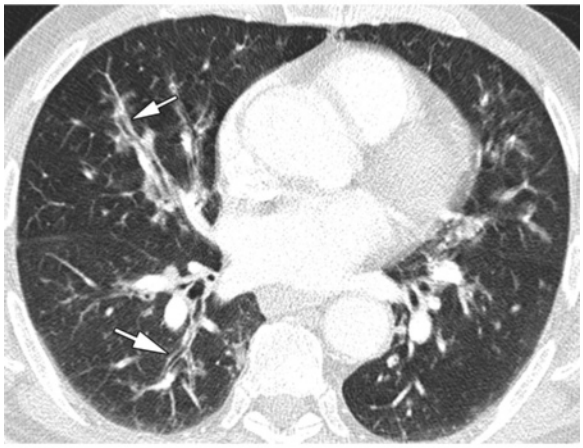

b.

Figure 13. CSS in a 72-year-old asthmatic man who presented with chronic cough and dyspnea. He had a history of persistent eosinophilia and sinus polyposis. CT images (lung window) show small centrilobular nodules (arrows in **a**) and diffuse bronchial wall thickening (arrows in **b**), with some areas of tree-in-bud pattern.

of patients (52). Interlobular septal thickening may reflect the presence of edema secondary to cardiac involvement or eosinophilic infiltration of the septa (50).

Airway involvement consisting of small centrilobular nodules and the tree-in-bud sign, bronchial dilatation, and bronchial and bronchiolar wall thickening (Figs 12, 13) (common CT findings in asthmatic patients) is likely to be related to asthma, which is almost always present in CSS (50,51). However, eosinophilic involvement of the bronchial wall may account for the bronchial wall thickening (51).

Unilateral or bilateral pleural effusions are seen at CT in 10%–50% of patients and may be caused by left-sided heart failure resulting from cardiomyopathy or by eosinophilic pleuritis. Less common manifestations include a diffuse reticular pattern or small and large nodular opacities that seldom cavitate (51).

In an asthmatic patient, when the radiograph shows areas of consolidation involving mainly the periphery of the lung, the main diagnostic considerations are chronic eosinophilic pneumonia, CSS, and organizing pneumonia. The diagnosis of CSS is based on systemic manifestations of CSS, including rash, peripheral neuropathy, and the presence of perinuclear ANCA in serum (seen in 35%–70% of patients with active disease) (53).

Microscopic Polyangiitis

Microscopic polyangiitis is a nongranulomatous necrotizing systemic vasculitis. It is the most common cause of pulmonary-renal syndrome, a syndrome characterized by the coexistence of pulmonary hemorrhage and glomerulonephritis (54). The clinical manifestations are usually renal and, less commonly, pulmonary. More than 90% of patients have rapidly progressive glomerulonephritis at presentation; diffuse pulmonary hemorrhage occurs in approximately 10%–30% of patients (7,9) and is present in nearly 30% at presentation (7). In patients who develop lung disease, DAH with pathologic capillaritis is the most common manifestation (2,55). Chest symptoms include hemoptysis and shortness of breath; other relatively common manifestations include skin lesions, peripheral neuritis, and gastrointestinal hemorrhage (2,9).

Radiographic findings in the various diseases causing diffuse pulmonary hemorrhage may be identical; these signs are described in the next section.

The diagnosis of microscopic polyangiitis should be suspected in patients with rapidly progressive glomerulonephritis in whom perinuclear ANCA is present and who show clinical and radiologic findings consistent with diffuse pulmonary hemorrhage. Clinically, the main differential diagnosis is with other conditions that may cause pulmonary and renal manifestations, particularly

Figure 14. Variety of chest radiographic features that can be found in DAH. **(a)** Wegener granulomatosis in a 62-year-old woman who presented with malaise and hemoptysis and had a positive test result for cytoplasmic ANCA. Chest radiograph shows bilateral hazy areas of increased opacity and areas of consolidation that are more prominent in the perihilar regions. **(b)** Systemic lupus erythematosus in a 35-year-old woman who presented with sudden dyspnea, coughing, hemoptysis, and anemia. Chest radiograph shows diffuse bilateral areas of consolidation.

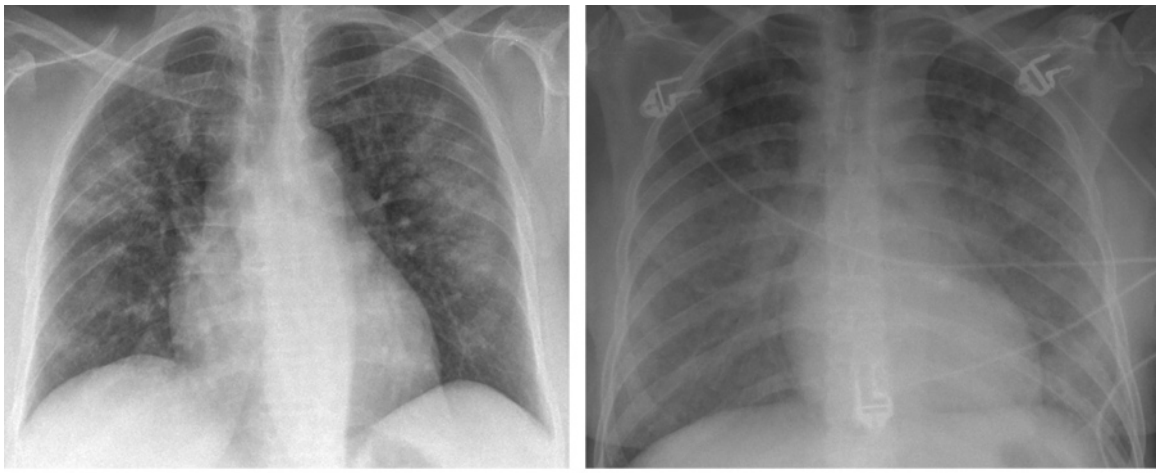

a. b.

Goodpasture syndrome (which is diagnosed by demonstration of circulating or tissue-bound anti–glomerular basement membrane antibodies), Wegener granulomatosis (granulomatous inflammation at surgical lung biopsy), and systemic lupus erythematosus (immune deposits at surgical lung biopsy) (56).

Diffuse Alveolar Hemorrhage

Teaching Point

DAH can be defined by the presence of hemoptysis, diffuse alveolar infiltrates, and a drop in hematocrit level. Symptoms include cough, hemoptysis, dyspnea, and anemia. However, chest radiographic and CT findings are nonspecific (the alveolar infiltrates can even sometimes be unilateral), and hemoptysis may be lacking (even in patients with sufficient hemorrhage to result in anemia) (2,7,57). The diagnosis is usually made with bronchoscopy, by means of which serial bronchoalveolar lavage samples (from the same location) reveal an increasing red blood cell count.

Whatever the underlying cause of DAH, the resultant hemorrhagic filling of the airspaces causes widespread radiographic shadowing, which ranges in intensity from vague ground-glass opacity to extensive intense consolidation (58,59).

The radiographic lung features consist of patchy or diffuse bilateral airspace opacities (Fig 14). The bilateral ground-glass opacities and consolidation are usually widespread but may be more prominent in the perihilar areas and in the mid and lower lung zones (58). The corresponding findings on thin-section CT images are equally nonspecific, with ground-glass opacity as the cardinal feature (Fig 15a). There is no characteristic distribution, and the opacities may be patchy or uniform. Ill-defined centrilobular nodules may predominate in some patients (Fig 15b). The presence of dense consolidation represents complete filling of the alveoli with blood (Fig 15c) (58,59).

Within days of an acute episode of hemorrhage, interlobular septal thickening may be seen in association with ground-glass opacity (crazy-paving pattern) as hemosiderin-laden macrophages accumulate in the interstitium (42,60) (Fig 15d). Unless further hemorrhage occurs, complete clearing of airspace and interstitial opacities usually occurs within 10 days to 2 weeks after an acute episode of hemorrhage. This is considerably slower than clearing of pulmonary edema, which hemorrhage closely resembles. After repeated episodes of pulmonary hemorrhage, a persistent reticular pattern may be seen, with

Figure 15. Variety of high-resolution CT patterns that can be found in DAH. **(a)** Microscopic polyangiitis in a 41-year-old man. CT image shows patchy areas of ground-glass opacity. **(b)** Microscopic polyangiitis in a 50-year-old woman who presented with cough and dyspnea. Results of bronchoalveolar lavage were positive for alveolar hemorrhage. CT image shows diffuse centrilobular nodules with no other abnormalities. **(c)** Wegener granulomatosis in a 62-year-old woman (same patient as in Fig 14a). CT image shows extensive areas of consolidation in a predominantly perihilar distribution. **(d)** Systemic lupus erythematosus in a 35-year-old woman (same patient as in Fig 14b). CT image shows diffuse ground-glass opacities, ill-defined centrilobular nodules, and septal thickening (arrows). **(e)** Microscopic polyangiitis in a 72-year-old woman. CT image obtained after recurrent episodes of pulmonary hemorrhage shows a fine reticular pattern on a background of ground-glass attenuation, signs of pulmonary fibrosis with a peripheral honeycombing pattern (arrows), and traction bronchiectasis (arrowhead).

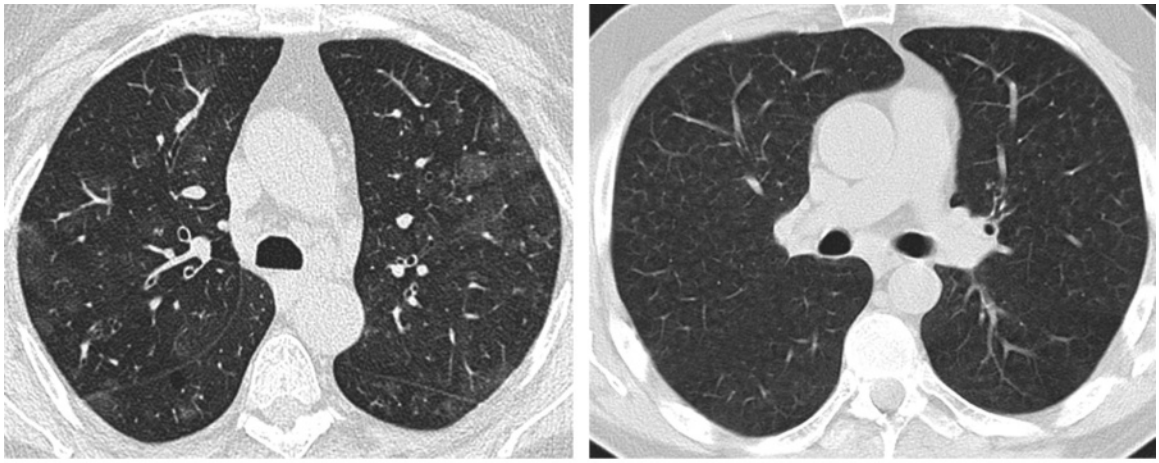

a.

b.

c.

d.

e.

areas of peripheral honeycombing and traction bronchiectasis; this pattern reflects interstitial hemosiderin deposition and mild lung fibrosis and has been termed *pulmonary hemosiderosis* (7,42,60) (Fig 15e). It may be seen in recurrent hemorrhage of any cause but is particularly common in patients with idiopathic pulmonary hemosiderosis (7).

The histopathologic differential diagnosis of DAH includes diseases associated with pulmonary capillaritis (a cellular infiltrate of neutrophils in the capillaries and venules) and those associated with normal vessels or bland hemorrhage (2,61) (Table 4). The many different entities causing DAH may be classified into three groups: *(a)* ANCA-associated small-vessel vasculitis, which generally involves pulmonary capillaritis (Wegener granulomatosis, CSS, microscopic polyangiitis); *(b)* syndromes caused by immune deposits that can be detected with immunofluorescence, such as Goodpasture syndrome and systemic lupus erythematosus; and *(c)* a large group of miscellaneous entities that includes diffuse alveolar damage, drug reactions (including cocaine inhalation), coagulopathies, infections, and idiopathic disease such as idiopathic pulmonary hemosiderosis (2,57,62). Most cases of DAH are caused by capillaritis associated with systemic autoimmune diseases such as ANCA-associated small-vessel vasculitis, Goodpasture syndrome, and systemic lupus erythematosus (2).

Pulmonary-renal syndrome is defined as the combination of DAH and glomerulonephritis. The differential diagnosis includes mainly the ANCA-associated vasculitides (70% of cases), Goodpasture syndrome, and systemic lupus erythematosus (2,7,9).

Goodpasture syndrome is extremely rare (one case per 1,000,000 people per year). It is defined by the presence of anti–glomerular basement membrane antibodies; these antibodies bind specifically to basement membrane antigens of the alveolus and glomerulus (9).

Clinically relevant DAH is a rare (2% of patients) but serious complication of systemic lupus erythematosus. The reported mortality rate for DAH in systemic lupus erythematosus is approximately 60%. Typically, patients present with symptoms of generalized systemic lupus erythematosus vasculitis, such as renal failure, arthritis, or a rash (7,63). DAH has also been reported in a small number of patients with other connective tissue disease, such as mixed connective tissue disease and rheumatoid arthritis.

Idiopathic pulmonary hemosiderosis is a rare disease of unknown origin characterized by recurrent episodes of diffuse pulmonary hemorrhage without associated glomerulonephritis or serologic abnormalities (58). Idiopathic pulmonary hemosiderosis most commonly occurs in

Table 4
Causes of DAH

With pathologic capillaritis
Primary idiopathic small-vessel vasculitis
Wegener granulomatosis
CSS
Microscopic polyangiitis
Primary immune complex–mediated vasculitis
Goodpasture syndrome
Henoch-Schönlein purpura
Secondary vasculitis
Classic autoimmune disease
Systemic lupus erythematosus
Rheumatoid arthritis
Antiphospholipid antibody syndrome
Mixed connective tissue disease
Polymyositis, dermatomyositis
Essential cryoglobulinemic vasculitis
Behçet disease
Lung transplantation
Bone marrow transplantation
Drug induced (eg, chemotherapy)
Infection
Without pathologic capillaritis
Idiopathic pulmonary hemosiderosis
Coagulopathy
Mitral stenosis
Inhalation injury
Goodpasture syndrome
Systemic lupus erythematosus
Bone marrow transplantation
Drug-associated disease (eg, chemotherapy)

Source.—References 2 and 7.

children or young adults. The diagnosis is usually made by exclusion (42,62).

DAH must be considered in patients with otherwise unexplained alveolar infiltrates, particularly when seen with a connective tissue disease (mainly systemic lupus erythematosus) or new-onset renal insufficiency (62). If the underlying cause remains uncertain after a careful clinical evaluation that includes imaging studies, serologic studies (for ANCA, anti–glomerular basement membrane antibodies, antinuclear antibody, circulating immunocomplexes, among others), and bronchoscopy, then surgical biopsy should be considered (64). Which organ to perform biopsy on (eg, lung, sinus, kidney) depends on the level of suspicion for a specific cause. The histopathologic presence of capillaritis suggests a systemic vasculitis as the underlying cause (64).

Diagnostic Approach

Teaching Point

The primary vasculitides are rare disorders, and their diagnoses are among the most demanding challenges in medicine because their signs and symptoms are nonspecific and overlap with those of infections, connective tissue diseases, and malignancies. An integrated clinical, radiologic, and sometimes histologic approach is needed. Symptoms such as uveitis, unusual rashes, arthritis, or "sinus troubles" must be remembered and considered relevant when the clinical presentation is an abnormal lung CT or chest radiographic finding, shortness of breath, or renal failure.

Large-vessel vasculitis (GCA and Takayasu arteritis) should be suspected when there are ischemic signs and symptoms. The main radiologic finding that should alert to large-vessel vasculitis is arterial wall thickening. Although histologically similar, GCA and Takayasu arteritis are considered distinct disease entities on the basis of age of onset, distribution of vascular involvement, and clinical presentation (24). Unlike GCA, Takayasu arteritis affects almost exclusively patients younger than 40 years, involves primarily the aorta and its major branches, and generally spares the cranial arteries. Behçet disease is the most common cause of pulmonary artery aneurysms; diagnosis of Behçet disease as the cause of pulmonary artery aneurysm is usually straightforward on the basis of the characteristic history of recurrent oral and genital ulcerations and uveitis.

Teaching Point

The presence of otherwise unexplained nodular or cavitary disease should raise the suspicion of vasculitis. Although infection and malignancy are the most common explanations, in the correct clinical setting vasculitis, particularly Wegener granulomatosis, should be strongly considered.

CSS should be suspected when patchy ground-glass opacities or consolidations are seen in a patient with a history of asthma who also presents with eosinophilia. Differentiation between CSS and simple pulmonary eosinophilia or chronic eosinophilic pneumonia in an asthmatic patient is based on systemic manifestations of CSS (eg, peripheral neuropathy, rash) and the presence of perinuclear ANCA in serum.

Radiologic signs of DAH are nonspecific and variable but must be considered in patients with otherwise unexplained alveolar infiltrates, particularly when seen with new-onset renal insufficiency or a connective tissue disease.

Conclusions

The diagnosis of vasculitis is often delayed because a number of other disorders can mimic the clinical manifestations. Chest radiographs and especially CT are valuable for noninvasive diagnosis in patients with pulmonary vasculitis; certain radiologic signs in combination with clinical features enable an earlier diagnosis.

Acknowledgments.—The authors thank Ricard Valero, MD, PhD, for technical support and John Giba for linguistic aid.

References

1. Heeringa P, Schreiber A, Falk RJ, Jennette JC. Pathogenesis of pulmonary vasculitis. Semin Respir Crit Care Med 2004;25(5):465–474.
2. Brown KK. Pulmonary vasculitis. Proc Am Thorac Soc 2006;3(1):48–57.
3. González-Gay MA, García-Porrúa C. Systemic vasculitis in adults in northwestern Spain, 1988-1997: clinical and epidemiologic aspects. Medicine 1999;78(5):292–308.
4. Watts RA, Lane SE, Bentham G, Scott DG. Epidemiology of systemic vasculitis: a ten-year study in the United Kingdom. Arthritis Rheum 2000;43(2):414–419.

5. Travis WD, Colby TV, Lombard C, Carpenter HA. A clinicopathologic study of 34 cases of diffuse pulmonary hemorrhage with lung biopsy confirmation. Am J Surg Pathol 1990;14:1112–1125.
6. Jennette JC, Falk RJ, Andrassy K, et al. Nomenclature of systemic vasculitides: proposal of an international consensus conference. Arthritis Rheum 1994;37(2):187–192.
7. Marten K, Schnyder P, Schirg E, Prokop M, Rummeny EJ, Engelke C. Pattern-based differential diagnosis in pulmonary vasculitis using volumetric CT. AJR Am J Roentgenol 2005;184:720–733.
8. Sorensen SF, Slot O, Tvede N, Petersen J. A prospective study of vasculitis patients collected in a five year period: evaluation of the Chapel Hill nomenclature. Ann Rheum Dis 2000;59:478–482.
9. Frankel SK, Cosgrove GP, Fischer A, Meehan RT, Brown KK. Update in the diagnosis and management of pulmonary vasculitis. Chest 2006;129:452–465.
10. Hagen EC, Daha MR, Hermans J, et al. Diagnostic value of standardized assays for anti-neutrophil cytoplasmic antibodies in idiopathic systemic vasculitis. EC/BCR Project for ANCA Assay Standardization. Kidney Int 1998;53(3):743–753.
11. Choi HK, Liu S, Merkel PA, Colditz GA, Niles JL. Diagnostic performance of antineutrophil cytoplasmic antibody tests for idiopathic vasculitides: metaanalysis with a focus on antimyeloperoxidase antibodies. J Rheumatol 2001;28(7):1584–1590.
12. Jennette JC, Falk RJ. Small-vessel vasculitis. N Engl J Med 1997;337(21):1512–1523.
13. Michel BA, Arend WP, Hunder GG. Clinical differentiation between giant cell (temporal) arteritis and Takayasu's arteritis. J Rheumatol 1996;23(1):106–111.
14. Matsunaga N, Hayashi K, Sakamoto I, Ogawa Y, Matsumoto T. Takayasu arteritis: protean radiologic manifestations and diagnosis. RadioGraphics 1997;17:579–594.
15. Johnston SL, Lock RJ, Gompels MM. Takayasu arteritis: a review. J Clin Pathol 2002;55:481–486.
16. Numano F, Okawara M, Inomata H, Kobayashi Y. Takayasu's arteritis. Lancet 2000;356:1023–1025.
17. Nastri MV, Baptista LPS, Baroni RH, et al. Gadolinium-enhanced three-dimensional MR angiography of Takayasu arteritis. RadioGraphics 2004;24:773–786.
18. Gotway MB, Araoz PA, Macedo TA, et al. Imaging findings in Takayasu's arteritis. AJR Am J Roentgenol 2005;184:1945–1950.
19. Park JH, Chung JW, Im JG, Kim SK, Park YB, Han MC. Takayasu arteritis: evaluation of mural changes in the aorta and pulmonary artery with CT angiography. Radiology 1995;196(1):89–93.
20. Desai MY, Stone JH, Foo TKF, et al. Delayed contrast-enhanced MRI of the aortic wall in Takayasu's arteritis: initial experience. AJR Am J Roentgenol 2005;184:1427–1431.
21. Meller J, Strutz F, Siefker U, et al. Early diagnosis and follow-up of aortitis with [(18)F]FDG PET and MRI. Eur J Nucl Med Mol Imaging 2003;30(5):730–736.
22. Salvarani C, Cantini F, Boiardi L, Hunder GG. Polymyalgia rheumatica and giant-cell arteritis. N Engl J Med 2002;347(4):261–271.
23. Lawrence RC, Felson DT, Helmick CG, et al. Estimates of the prevalence of arthritis and other rheumatic conditions in the United States. Part II. Arthritis Rheum 2008;58(1):26–35.
24. Tatò F, Hoffmann U. Giant cell arteritis: a systemic vascular disease. Vasc Med 2008;13(2):127–140.
25. Evans JM, O'Fallon WM, Hunder GG. Increased incidence of aortic aneurysm and dissection in giant cell (temporal) arteritis: a population-based study. Ann Intern Med 1995;122:502–507.
26. Evans JM, Bowles CA, Bjornsson J, Mullany CJ, Hunder GG. Thoracic aortic aneurysm and rupture in giant cell arteritis: a descriptive study of 41 cases. Arthritis Rheum 1994;37:1539–1547.
27. Yun M, Yeh D, Arujo LI, Jang S, Newberg A, Alavi A. F-18 FDG uptake in the large arteries: a new observation. Clin Nucl Med 2001;26:314–319.
28. Walter MA. [^{18}F] Fluorodeoxyglucose PET in large vessel vasculitis. Radiol Clin North Am 2007;45(4):735–744.
29. Erkan F, Gül A, Tasali E. Pulmonary manifestations of Behçet's disease. Thorax 2001;56:572–578.
30. Hiller N, Lieberman S, Chajek-Shaul T, Bar-Ziv J, Shaham D. Thoracic manifestations of Behçet disease at CT. RadioGraphics 2004;24:801–808.
31. Chae EJ, Do KH, Seo JB, et al. Radiologic and clinical findings of Behçet disease: comprehensive review of multisystemic involvement. RadioGraphics 2008;28(5):e31.
32. Tunaci M, Ozkorkmaz B, Tunaci A, Gul A, Engin G, Acunas B. CT findings of pulmonary artery aneurysms during treatment for Behçet's disease. AJR Am J Roentgenol 1999;172:729–733.
33. Hamuryudan V, Yurdakul S, Moral E, et al. Pulmonary arterial aneurysms in Behçet's syndrome: a report of 24 cases. Br J Rheumatol 1994;33:48–51.
34. Mogulkoc N, Burgess MI, Bishop PW. Intracardiac thrombus in Behçet's disease: a systematic review. Chest 2000;118:479–487.
35. Frankel SK, Sullivan EJ, Brown KK. Vasculitis: Wegener granulomatosis, Churg-Strauss syndrome, microscopic polyangiitis, polyarteritis nodosa, and Takayasu arteritis. Crit Care Clin 2002;18(4):855–879.
36. Jennette JC, Falk RJ. Nosology of primary vasculitis. Curr Opin Rheumatol 2007;19(1):10–16.

37. Luqmani RA, Bacon PA, Beaman M, et al. Classical versus non-renal Wegener's granulomatosis. Q J Med 1994;87(3):161–167.
38. Travis WD, Hoffman GS, Leavitt RY, Pass HI, Fauci AS. Surgical pathology of the lung in Wegener's granulomatosis: review of 87 open lung biopsies from 67 patients. Am J Surg Pathol 1991; 15(4):315–333.
39. Lee KS, Kim TS, Fujimoto K, et al. Thoracic manifestation of Wegener's granulomatosis: CT findings in 30 patients. Eur Radiol 2003;13(1):43–51.
40. Lohrmann C, Uhl M, Kotter E, Burger D, Ghanem N, Langer M. Pulmonary manifestations of Wegener granulomatosis: CT findings in 57 patients and a review of the literature. Eur J Radiol 2005;53(3): 471–477.
41. Komócsi A, Reuter M, Heller M, Muraközi H, Gross WL, Schnabel A. Active disease and residual damage in treated Wegener's granulomatosis: an observational study using pulmonary high-resolution computed tomography. Eur Radiol 2003; 13(1):36–42.
42. Remy-Jardin M, Remy J, Mayo JR, Müller NL. Diffuse pulmonary hemorrhage and pulmonary vasculitis. In: CT angiography of the chest. Philadelphia, Pa: Lippincott Williams & Wilkins, 2001; 488–497.
43. Ananthakrishnan L, Sharma N, Kanne JP. Wegener's granulomatosis in the chest: high-resolution CT findings. AJR Am J Roentgenol 2009;192(3): 676–682.
44. Franks TJ, Koss MN. Pulmonary capillaritis. Curr Opin Pulm Med 2000;6:430–435.
45. Müller NL, Silva CIS. Wegener granulomatosis. In: Müller NL, Silva CIS, eds. Imaging of the chest. Philadelphia, Pa: Saunders-Elsevier, 2008; 811–819.
46. Masi AT, Hunder GG, Lie JT, et al. The American College of Rheumatology 1990 criteria for the classification of Churg-Strauss syndrome (allergic granulomatosis and angiitis). Arthritis Rheum 1990;33(8):1094–1100.
47. Choi YH, Im JG, Han BK, Kim JH, Lee KY, Myoung NH. Thoracic manifestation of Churg-Strauss syndrome: radiologic and clinical findings. Chest 2000;117(1):117–124.
48. Solans R, Bosch JA, Pérez-Bocanegra C, et al. Churg-Strauss syndrome: outcome and long-term follow-up of 32 patients. Rheumatology 2001;40: 763–771.
49. Katzenstein AL. Diagnostic features and differential diagnosis of Churg-Strauss syndrome in the lung: a review. Am J Clin Pathol 2000;114:767–772.
50. Kim YK, Lee KS, Chung MP, et al. Pulmonary involvement in Churg-Strauss syndrome: an analysis of CT, clinical, and pathologic findings. Eur Radiol 2007;17:3157–3165.
51. Silva CI, Müller NL, Fujimoto K, Johkoh T, Ajzen SA, Churg A. Churg-Strauss syndrome: high resolution CT and pathologic findings. J Thorac Imaging 2005;20(2):74–80.
52. Worthy SA, Müller NL, Hansell DM, et al. Churg-Strauss syndrome: the spectrum of pulmonary CT findings in 17 patients. AJR Am J Roentgenol 1998;170:297–300.
53. Silva CI, Müller NL. Churg-Strauss syndrome. In: Müller NL, Silva CIS, eds. Imaging of the chest. Philadelphia, Pa: Saunders-Elsevier, 2008; 821–827.
54. Bosch X, Guilabert A, Font J. Antineutrophil cytoplasmic antibodies. Lancet 2006;368(9533):404–418.
55. Akikusa B, Sato T, Ogawa M, Ueda S, Kondo Y. Necrotizing alveolar capillaritis in autopsy cases of microscopic polyangiitis: incidence, histopathogenesis and relationship with systemic vasculitis. Arch Pathol Lab Med 1997;121:144–149.
56. Silva CI, Müller NL. Microscopic polyangiitis. In: Müller NL, Silva CIS, eds. Imaging of the chest. Philadelphia, Pa: Saunders-Elsevier, 2008; 834–837.
57. Green RJ, Ruoss SJ, Kraft SA, Duncan SR, Berry GJ, Raffin TA. Pulmonary capillaritis and alveolar hemorrhage: update on diagnosis and management. Chest 1996;110(5):1305–1316.
58. Primack SL, Miller RR, Müller NL. Diffuse pulmonary hemorrhage: clinical, pathologic, and imaging features. AJR Am J Roentgenol 1995;164(2): 295–300.
59. Hansell DM. Small-vessel diseases of the lung: CT-pathologic correlates. Radiology 2002;225(3):639–653.
60. Ando Y, Okada F, Matsumoto S, Mori H. Thoracic manifestation of myeloperoxidase-antineutrophil cytoplasmic antibody (MPO-ANCA)-related disease: CT findings in 51 patients. J Comput Assist Tomogr 2004;28(5):710–716.
61. Mark EJ, Ramirez JF. Pulmonary capillaritis and hemorrhage in patients with systemic vasculitis. Arch Pathol Lab Med 1985;109(5):413–418.
62. Ioachimescu OC, Sieber S, Kotch A. Idiopathic pulmonary haemosiderosis revisited. Eur Respir J 2004;24:162–170.
63. Zamora MR, Warner ML, Tuder R, et al. Diffuse alveolar hemorrhage in systemic lupus erythematosus: clinical presentation, histology, survival and outcome. Medicine 1997;76:192–202.
64. Ioachimescu OC. Alveolar hemorrhage. In: Laurent GL, Shapiro SD, eds. Encyclopedia of respiratory medicine. Amsterdam, the Netherlands: Academic Press, 2006; 92–100.

This article meets the criteria for 1.0 credit hour in category 1 of the AMA Physician's Recognition Award. To obtain credit, see accompanying test at http://www.rsna.org/education/rg_cme.html.

When to Suspect Pulmonary Vasculitis: Radiologic and Clinical Clues

Eva Castañer, MD, et al

RadioGraphics 2010; 30:33–53 • **Published online** 10.1148/rg.301095103 • **Content Codes:** CH CT

Page 35
ANCAs are antibodies against intracellular antigens found in neutrophils and monocytes. The ANCA-associated vasculitides (Wegener granulomatosis, CSS, and microscopic polyangiitis) are grouped together because of common clinical features, histopathologic involvement of small vessels, similar response to immunosuppressive treatment, and ANCA positivity (9). ANCA positivity is common in these entities but not universal; thus, ANCA negativity does not completely rule out these diseases.

Page 38
Extracranial involvement is probably underdiagnosed in patients with classic GCA or mistaken for arteriosclerotic disease in patients without temporal arteritis or typical symptoms of GCA. Extracranial GCA has most frequently been reported in the aortic arch and the subclavian and axillary arteries (22,24). At histologic analysis, GCA appears similar to Takayasu arteritis (24). The principal CT and MR imaging appearance of GCA is similar to that of Takayasu arteritis, with evidence of arterial wall thickening (Fig 5), stenosis, and aneurysm (7). Aortic GCA typically remains asymptomatic during the early phase of the disease and causes serious late complications like aneurysms and dissections.

Page 48
DAH can be defined by the presence of hemoptysis, diffuse alveolar infiltrates, and a drop in hematocrit level. Symptoms include cough, hemoptysis, dyspnea, and anemia. However, chest radiographic and CT findings are nonspecific (the alveolar infiltrates can even sometimes be unilateral), and hemoptysis may be lacking (even in patients with sufficient hemorrhage to result in anemia) (2,7,57). The diagnosis is usually made with bronchoscopy, by means of which serial bronchoalveolar lavage samples (from the same location) reveal an increasing red blood cell count. Whatever the underlying cause of DAH, the resultant hemorrhagic filling of the airspaces causes widespread radiographic shadowing, which ranges in intensity from vague ground-glass opacity to extensive intense consolidation (58,59).

Page 51
The primary vasculitides are rare disorders, and their diagnoses are among the most demanding challenges in medicine because their signs and symptoms are nonspecific and overlap with those of infections, connective tissue diseases, and malignancies. An integrated clinical, radiologic, and sometimes histologic approach is needed. Symptoms such as uveitis, unusual rashes, arthritis, or "sinus troubles" must be remembered and considered relevant when the clinical presentation is an abnormal lung CT or chest radiographic finding, shortness of breath, or renal failure.

Page 51
The presence of otherwise unexplained nodular or cavitary disease should raise the suspicion of vasculitis. Although infection and malignancy are the most common explanations, in the correct clinical setting vasculitis, particularly Wegener granulomatosis, should be strongly considered.